

# Unveiling Sophisticated Intermolecular van der Waals Interactions at the Single-Molecule Level

Haiyang Ren,<sup>†</sup> Peihui Li,<sup>†</sup> Jie Hao,<sup>†</sup> Wan Xiong,<sup>†</sup> Linqi Pei, Boyu Wang, Cong Zhao, Suhang He, Shan Jin,\* Jingtao Lü,\* Jinying Wang,\* Chuancheng Jia,\* and Xuefeng Guo\*



Cite This: *ACS Materials Lett.* 2025, 7, 754–760



Read Online

ACCESS |



Metrics & More

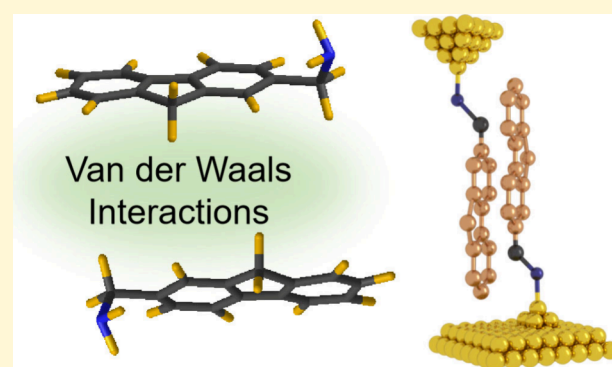


Article Recommendations



Supporting Information

**ABSTRACT:** Weak yet ubiquitous van der Waals (vdW) interactions play an essential role in shaping the structure, stability, and functionality of materials. Particularly, intermolecular vdW interactions profoundly impact molecular stacking orders and electronic properties. However, comprehending and precisely controlling intermolecular vdW interactions has posed a long-standing challenge. Here, we employ a combination of single-molecule electrical measurements and theoretical calculations to dissect and further regulate sophisticated vdW interactions in a single-dimer junction. Specifically, by introducing an aminomethyl group, the electrostatic force resulting from the dipole–dipole interaction predominantly dictates the bistable conformation and conductance of benzylamine dimers. As molecular  $\pi$ -conjugation increases, the influence of exchange and dispersion interactions is significantly amplified in (9H-fluoren-2-yl)methylamine dimers. Furthermore, the application of electric fields effectively modulates the vdW interactions in dimers, impacting their structures and conductance. Investigating these vdW interactions yields profound insights into the fundamental principles governing the behavior of chemical and biological systems.



Weak yet fundamental van der Waals (vdW) interactions (typically ranging from 0.5 to 3 kcal mol<sup>-1</sup>) profoundly influence molecules and materials, shaping their structures and electronic properties.<sup>1,2</sup> Van der Waals interactions, which include orientation, induction, dispersion, and exchange forces, are pervasive in conjugated molecules,<sup>3,4</sup> supramolecules,<sup>5</sup> two-dimensional materials,<sup>6</sup> and metal/organic interfaces.<sup>7,8</sup> Exploring these interactions, particularly intermolecular interactions, is essential for unraveling structure–function relationships and expanding applications in molecular electronics,<sup>9–13</sup> material self-assembly,<sup>14,15</sup> and organic synthesis.<sup>2,16,17</sup>

Precisely exploring and regulating intermolecular vdW interactions, especially various vdW interaction components, is challenging. Previous studies have indicated that dispersion interaction plays a critical role in benzene dimers<sup>18,19</sup> and other clusters of aromatic molecules<sup>20,21</sup> through ab initio calculations and nuclear magnetic resonance or rotational spectroscopic experiments.<sup>22</sup> However, the macroscopic experiments are difficult to eliminate the influence of molecular ensembles and finely regulate vdW interactions. Meanwhile, single-molecule junction technologies,<sup>23</sup> such as dynamic

scanning tunneling microscopy break junction (STM-BJ) and static graphene-based single-molecule junction, have been employed to investigate the vdW interactions between molecules and electrodes,<sup>8,12</sup> as well as other noncovalent interactions in molecular dimers, including  $\pi$ – $\pi$  interactions,<sup>9,11,24</sup>  $\sigma$ – $\sigma$  interactions<sup>25</sup> and hydrogen bonds,<sup>26</sup> owing to their high sensitivity of charge transport properties to dimer configurations. The single-molecule junctions serve as an ideal platform for exploring the weak yet ubiquitous intermolecular interactions.

Conjugated molecular dimers are typical systems for studying intermolecular vdW interactions. Previous studies on vdW interactions have focused on purely theoretical analyses<sup>27</sup> or purely experimental investigations of individual

Received: January 7, 2025

Revised: January 24, 2025

Accepted: January 27, 2025

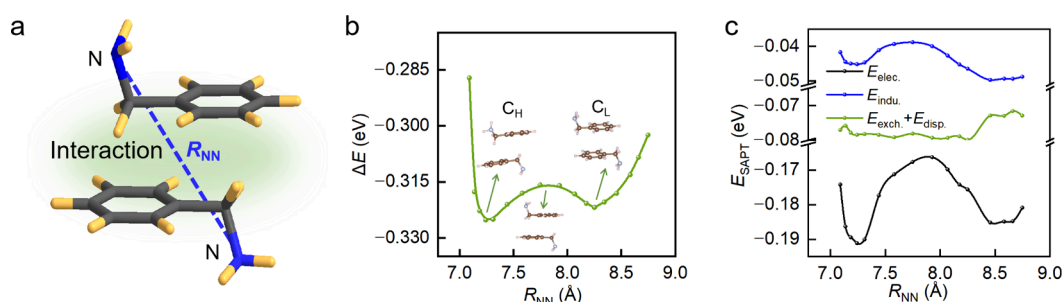


**Figure 1.** Van der Waals interactions in benzylamine dimers. (a) Schematic diagram for intermolecular vdW interactions in benzylamine dimers. (b) Theoretical predictions for the total intermolecular vdW interaction energy as a function of the inter-monomer distance in the parallel direction. (c) Energy difference of interaction energy components including electrostatic, induction, exchange and dispersion terms as a function of the inter-monomer distance calculated by SAPT.

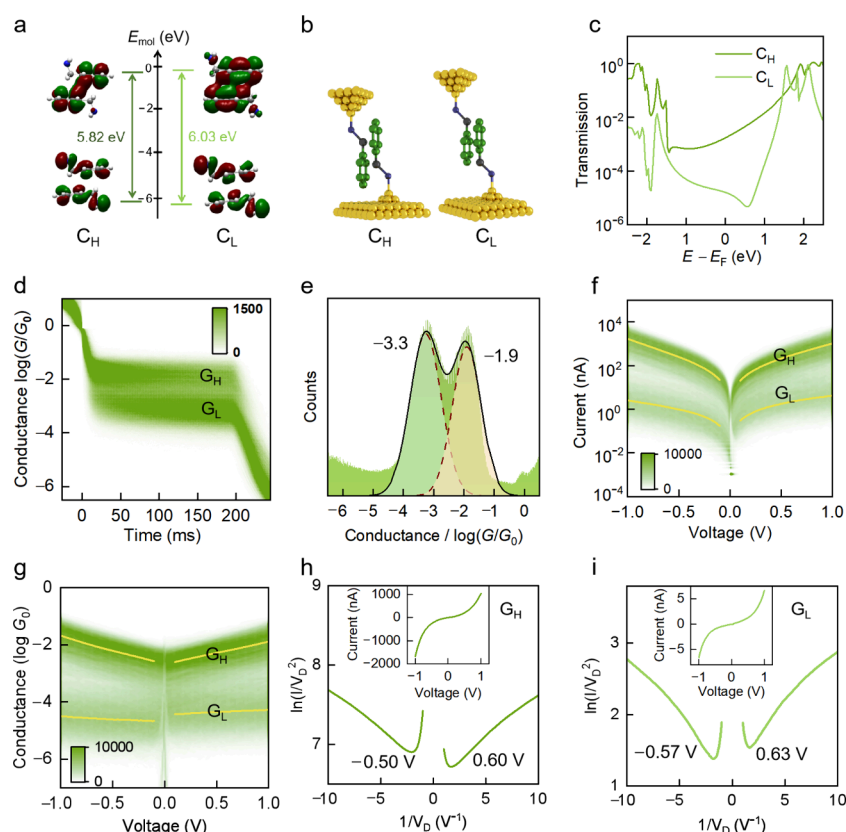


**Figure 2.** Charge transport through suspended benzylamine molecular junctions. (a) Calculated molecular energy levels and related molecular orbital diagrams of two stable states. (b) Schematic illustration of two stable states of benzylamine dimer in STM-BJ measurements. (c) Theoretical transmission spectra of benzylamine dimer with different stable states. (d) 2D conductance histograms of traces with the suspended retracting process under 0.1 V bias. (e) Corresponding 1D conductance histograms of traces. (f) 2D current versus voltage ( $I$ - $V$ ) histograms of benzylamine junctions. (g) 2D conductance versus voltage ( $dI/dV$ - $V$ ) histograms of benzylamine junctions. The yellow line represents the most representative current value from the Gaussian fitting. (h,i) Fowler–Nordheim plots of high conductance state (h) and low conductance state (i), respectively. The transition voltages for positive and negative polarities are marked out. The insets show the corresponding  $I$ - $V$  curve on a linear scale.

forces,<sup>9,10</sup> such as electrostatic interactions. Here, our work combines the STM-BJ measurements and symmetry-adapted perturbation theory (SAPT) analysis to dissect and further regulate the various intermolecular vdW interactions in a single conjugated dimer junction. By monitoring the electrical conductance state and energy component analysis, the influence of different vdW interactions on the stability of dimers is explored. Specifically, the dominant interaction component of stable benzylamine dimers is regulated by introducing an aminomethyl group into common benzene

molecules. Furthermore, the investigation is extended to higher-conjugated molecules, aiming to understand how the vdW interaction components change with conjugation. Finally, the effect of an electric field on the modulation of vdW interactions and conductance states in the single-dimer junction is examined.

Benzylamine (Figure S1a), which is a common precursor in organic chemistry, is selected as a simple model system to investigate the vdW interactions within molecular dimers, denoted as B-NH<sub>2</sub> (Figure 1a). The unique composition of the

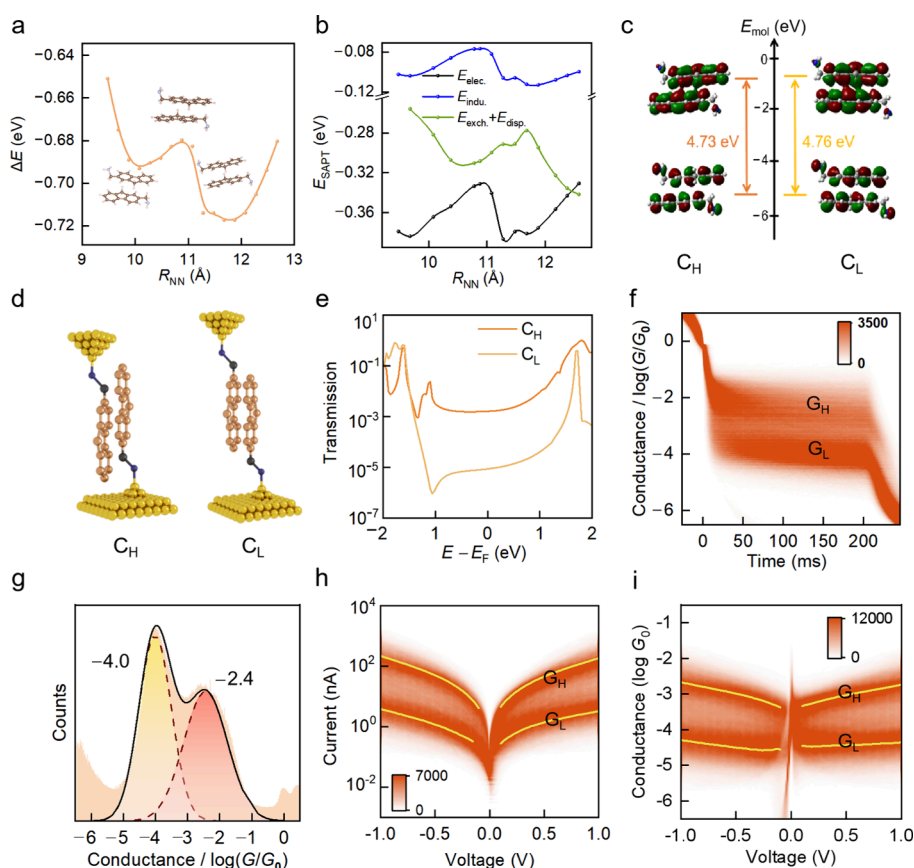


**Figure 3.** Charge transport through suspended F-NH<sub>2</sub> molecular junctions. (a) Theoretical predictions for the total intermolecular vdW interaction energy as a function of the distance between two F-NH<sub>2</sub> monomers in the parallel direction. (b) Energy difference for SAPT components (electrostatics, induction, exchange and dispersion terms) as a function of the distance between two F-NH<sub>2</sub> monomers in the parallel direction. (c) Calculated molecular energy levels and related molecular orbital diagrams of two stable states of F-NH<sub>2</sub> dimer. (d) Schematic illustration of two stable states of F-NH<sub>2</sub> dimer in STM-BJ measurements. (e) Theoretical transmission spectra of F-NH<sub>2</sub> dimer with different stable states. (f) 2D conductance histograms of traces with the suspended retracting process under 0.1 V bias. (g) Corresponding 1D conductance histograms of traces. (h) 2D  $I$ - $V$  histograms of F-NH<sub>2</sub> junctions. (i) 2D  $dI/dV$ - $V$  histograms of F-NH<sub>2</sub> junctions. The yellow line represents the most representative current value from the Gaussian fitting.

molecule, featuring an aromatic ring and an aminomethyl group, renders it to exhibit a weak dipole moment. It can be observed that the intermolecular vdW interactions in benzylamine dimers  $\Delta E = E_{\text{dimer}} - 2E_{\text{monomer}}$  vary with the distance between the two N atoms  $R_{\text{NN}}$  (Figure 1b). Two stable conformations with different stacking modes, C<sub>H</sub> and C<sub>L</sub>, are found. To uncover the nature of the intermolecular vdW interactions between molecules, SAPT analysis,<sup>27,28</sup> which provides a robust energy decomposition into physical components ( $E_{\text{SAPT}} = E_{\text{elec.}} + E_{\text{indu.}} + E_{\text{exch.}} + E_{\text{disp.}}$ ), is conducted (Figure S2 and S3). As shown in Figure 1c, the electrostatic component  $E_{\text{elec.}}$ , which originates from the permanent molecular dipole interaction, plays a dominant role in generating the two stable conformations, while for pure benzene dimer, the dispersion interaction would predominate.<sup>29,30</sup> The difference is due to the contribution of aminomethyl group. To be noted, the curve of interaction versus distance based on rigid scanning is smooth,<sup>30</sup> while we adopt relax scanning which gives less smooth curve but more accurate and richer information in the SAPT calculation (see the rigid scanning for comparison in Figure S4). The overlapping map of electrostatic potential (ESP)<sup>31</sup> provides an intuitive and rigorous explanation for the preference of dimer configurations, where the positive and negative parts of

ESP regions of each B-NH<sub>2</sub> monomer overlap more with each other in the two stable dimer configurations (Figure S5). The induction part  $E_{\text{indu.}}$  shows a similar but weaker effect as  $E_{\text{elec.}}$ . In contrast, the contributions of exchange and dispersion terms  $E_{\text{exch.}} + E_{\text{disp.}}$  to the relative stability of dimer stackings are nearly balanced out.

The two stable conformations of benzylamine dimer induced by varied vdW interactions have distinct electronic characteristics. Molecular frontier orbital analysis shows that the energy gap of the stable dimer configuration with larger-overlapped aromatic rings (C<sub>L</sub>) is relatively larger, and vice versa (Figure 2a). Because electrical conductance of a single-molecule junction is highly sensitive to its molecular conformation, the theoretical simulations and STM-BJ experiments (Section S1) are combined to measure the conformational transition of benzylamine dimer (Figure 2b). Benzylamine dimer junctions can be formed due to the strong binding of each monomer with Au tip or substrate through the -NH<sub>2</sub> anchor, so current flows through the dimer via intermolecular interaction. The calculated quantum transport properties of the benzylamine dimer junctions indicate over 1 order of magnitude difference of conductance for the two stable dimer stackings (Figure 2c). The conductance of dimer junctions is also experimentally measured as a function of tip-

substrate displacement to generate conductance versus displacement traces. Specifically, the single-dimer junctions are formed and broken in the solution of 1,2,4-trichlorobenzene (TCB). In order to avoid the influence of mechanical forces,<sup>9,12</sup> hovering experiments are performed to obtain richer information about the interaction forces of stable conformations. The tip is suspended during the retracting process for 150 ms after the formation of molecular junctions and collected  $\sim 10000$  traces in different cycles. The typical individual traces for the suspended molecular junction under 0.1 V bias are presented in Figure S6 and the conductance features of integer multiples of  $G_0$  ( $G_0 = 2 e^2/h$ ) can be observed. After the Au atomic contact is broken, the conductance shows rapid tunneling decay. Thousands of such conductance traces are used to construct the conductance histograms (Figure 2d). In addition, since the energy difference between the two stabilized conformations (Figure 1b) is very small, switching between the two states also occurs in the hovering experiments, as shown in Figure S7.

Two distinct conductance peaks are observed from the two-dimensional (2D) conductance histograms (Figure 2d) and the one-dimensional (1D) histograms (Figure 2e). The high conductance peak locates at  $\approx 1.3 \times 10^{-2} G_0$  ( $\approx 975.7$  nS) and the low conductance peak locates at  $\approx 5.0 \times 10^{-4} G_0$  ( $\approx 38.8$  nS), whose differences are consistent with the calculated transmission spectra. These results reveal that the high and low conductance states ( $G_H$  and  $G_L$ ) originate from the two conformations of dimer ( $C_H$  and  $C_L$ ), respectively. We attribute these two conductance states,  $G_H$  and  $G_L$ , to different stacking configurations of dimer junctions. This mechanism is supported by previous studies on the benzenethiol<sup>25</sup> and 1-methylimidazole dimer<sup>32</sup> junctions. In order to exclude the effect of the benzene ring in the TCB solvent on the conductance, we did a hovering experiment of TCB without the target molecule and found no obvious conductance peaks (Figure S8). Furthermore, a B-NH<sub>2</sub> dimer locked by carbon chains (Figure S1c) is introduced as a control system. Through the suspended retraction process by STM-BJ experiments, the B-NH<sub>2</sub> locked dimer junctions show conductance (Figure S9) nearly identical to the  $C_L$  state of B-NH<sub>2</sub> dimer junctions (Figure 2d), corresponding to the configuration with two locked benzenes stacking in parallel.

In addition, the current versus voltage ( $I-V$ ) (Figure 2f) and conductance versus voltage ( $dI/dV-V$ , where  $dI/dV$  is calculated from the  $I/V$  data) (Figure 2g) characteristics are investigated, too. Specifically, the  $I-V$  characterizations are implemented by suspended junctions when the corresponding conductance plateau is formed during the break junction measurement and scanning the bias voltage from  $-1.0$  to  $1.0$  V with a step of  $0.0005$  V. The collected  $I-V$  traces are used to construct 2D  $I-V$  histograms. The  $I-V$  measurements also support two stable states in benzylamine dimer. Meanwhile, from the Fowler–Nordheim plot ( $\ln(I/V^2)$  versus  $1/V$ ), it can be observed that the minimum value of transition voltage spectra (TVS) of  $G_H$  is smaller than that of  $G_L$  (Figure 2h,i). This corresponds to the molecular orbital simulation results that the highest occupied molecular orbital (HOMO) of the  $C_H$  is closer to the Fermi energy level of the electrodes than  $C_L$  state (Figure 2a).

Modulating the conjugated degree of monomers can not only regulate their own properties, but also affect the vdW interaction of dimers. For example, a fluorene-centered molecule named as F-NH<sub>2</sub> (Figure S1b) possesses more

aromatic rings compared to benzylamine, and thus might have stronger dispersion plus exchange interactions. Previous work has performed the molecular interactions of fluorene dimer through a combined rotational spectroscopic and quantum chemical study and has proven that the fluorene dimer is dominated by dispersion interactions.<sup>22</sup> However, when the aminomethyl group exists, the electrostatic and induction interactions also get enhanced. The intermolecular vdW interaction of F-NH<sub>2</sub> dimer as a function of the distance between two monomers are shown in Figure 3a, representing two stable dimer configurations. Compared to B-NH<sub>2</sub> dimer, the binding energy of F-NH<sub>2</sub> dimer is stronger, and the interaction of dispersion and exchange cannot be ignored. The overlapping map of electrostatic potential (ESP) provide intuitive and rigorous explanations for the stability of dimer configurations, where the positive and negative parts of ESP regions of each F-NH<sub>2</sub> monomer overlap more with each other in the two stable dimer configurations than other configurations (Figure S10). It can be observed that all the electrostatics, induction, exchange and dispersion jointly lead to the two stable states (Figure 3b; Figure S11). The molecular frontier orbital analysis shows different results with those of B-NH<sub>2</sub> dimer that the energy gap and molecular orbitals of the two stable configurations of F-NH<sub>2</sub> dimer are nearly the same (Figure 3c). The charge transport of F-NH<sub>2</sub> dimer has also been detected by a STM-BJ technique (Figure 3d) and theoretical simulations (Figure 3e). Two conductance states can be observed from the typical single trace (Figure S12), the 2D conductance–displacement histograms (Figure 3f) and the 1D histogram (Figure 3g) of the suspended F-NH<sub>2</sub> junctions. Furthermore, the current versus voltage ( $I-V$ ) (Figure 3h) and conductance versus voltage ( $dI/dV-V$ ) (Figure 3i) characteristics also show the bistate feature. To further investigate the origin of these differences, the transmission pathways at the Fermi level are calculated. As shown in Figure S13, the  $C_L$  state of F-NH<sub>2</sub> dimer exhibits significantly greater reflection than the  $C_H$  state, leading to a lower transmission coefficient and therefore lower conductance. Specifically, the  $\Delta E$  of  $C_L$  is lower than  $C_H$ , which means that the low state of F-NH<sub>2</sub> dimer is more stable, resulting in higher probability of low conductance in break junction experiments (Figure 3a, g). However, the occurrence probability of the two states of B-NH<sub>2</sub> dimer is almost identical, probably because the energy difference between the two states of B-NH<sub>2</sub> dimer is very small ( $\sim 0.0015$  eV), while the two states of F-NH<sub>2</sub> dimer have a large energy difference ( $\sim 0.03$  eV).

Previous studies have proven that electric fields can be used to regulate the conductance of molecular dimers.<sup>10</sup> Here, to investigate the regulation of intermolecular vdW interaction by an electric field, the bias dependent experiments on a suspended F-NH<sub>2</sub> junction have been conducted (Figure S14). In specific, the junction-forming probability of the low conductance state is higher than that of the high conductance state under a small bias voltage. As the bias increases, the relative probability ratio of the high conductance state to the low conductance state increases (Figure 4a), leading to a case where the probability of the low conductance state is lower than that of the high conductance state finally. This is consistent with the theoretical calculated energy difference of high and low conductance states under the electric field. Specifically, the energy difference between high and low states changes from positive to negative as the electric field increases (Figure 4b). This means that as the electric field increases, the

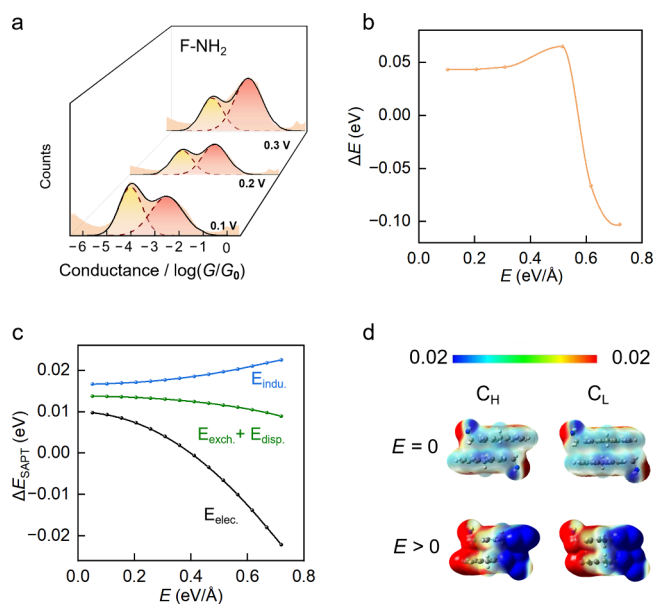


**Figure 4.** Regulation of vdW interaction of F-NH<sub>2</sub> dimer by an electric field. (a) 1D conductance histograms at different potentials of 0.1, 0.2, and 0.3 V. (b) Energy difference of the theoretically calculated high- and low-conductance configurations of F-NH<sub>2</sub> dimer, which varies with the electric field. (c) SAPT component energy difference ( $\Delta E_{\text{SAPT}} = E_{\text{SAPT}}(E > 0) - E_{\text{SAPT}}(E = 0)$ ) of the two configurations of F-NH<sub>2</sub> dimer under different electric fields. (d) Calculated electrostatic potential mapping of the two stable states of F-NH<sub>2</sub> dimer without/under (Up/Bottom panel) an electric field ( $E = 0.77$  eV/Å). The blue color represents the positive charge, while the red color represents the negative charge. ESP unit: Hartree/e.

high state becomes more stable than the low state, leading to an increasing proportion of the high conductance state. Furthermore, among the SAPT components, the dominant force causing this case is the electrostatic force, which also goes from positive to negative as the electric field increases (Figure 4c). This can be supported by the calculated electrostatic potential mapping (Figure 4d) of the two stable states of F-NH<sub>2</sub> dimer under an electric field. When the electric field is applied, the calculated electrostatic potential mapping show that the potential difference between the different parts of F-NH<sub>2</sub> dimer becomes larger, illustrating that the contribution of electrostatic interaction become more significant. In comparison with F-NH<sub>2</sub> dimer, the conductance states of B-NH<sub>2</sub> dimer show minimal changes with increasing bias (Figure S15) as their relative energy difference remains negative and varies only slightly (Figure S16).

In summary, we have investigated various intermolecular vdW interactions of single-dimer junctions using a sensitive STM-BJ technique in combination with SAPT analyses. Through monitoring the electrical conductance and tailoring the energy components, two stable conductance states in the single-dimer junction are found, corresponding to the different stacking configurations. Electrostatics and induction interactions are the dominant forces controlling the formation of the two stable states of benzylamine dimer, and the high conductance state is more stable than the other. As the molecular conjugation increases, the influence of exchange and dispersion interactions enhances in a fluorene-centered dimer. Furthermore, the electric field can be used to regulate the conductance states and vdW interactions of the dimers. These

findings offer valuable insights into comprehending, manipulating and designing intermolecular vdW interactions that influence the molecular stacking and assembly processes.

## ■ ASSOCIATED CONTENT

### Supporting Information

The Supporting Information is available free of charge at <https://pubs.acs.org/doi/10.1021/acsmaterialslett.5c00047>.

Experimental section, molecular structures, total vdW interaction energies of B-NH<sub>2</sub> dimer calculated by symmetry-adapted perturbation theory (SAPT) and Gaussian methods, calculated SAPT components of B-NH<sub>2</sub> dimer by relax scanning, calculated SAPT components of B-NH<sub>2</sub> dimer by rigid scanning, overlapping map of electrostatic potential of B-NH<sub>2</sub> dimer, typical suspended single traces of B-NH<sub>2</sub> dimer, typical suspended single traces of B-NH<sub>2</sub> dimer switching, the control experimental results without the target molecule, charge transport through suspended B-NH<sub>2</sub> locked dimer junctions, overlapping map of electrostatic potential of F-NH<sub>2</sub> dimer, calculated SAPT component energies of F-NH<sub>2</sub> dimer, typical suspended single traces of F-NH<sub>2</sub> dimer, transmission pathway of two stabilized conformations of F-NH<sub>2</sub> dimer at the Fermi energy level, bias dependence of the molecule F-NH<sub>2</sub>, bias dependence of the molecule B-NH<sub>2</sub>, calculated energy difference of the high- and low-conductance configurations of B-NH<sub>2</sub> dimer (PDF)

## ■ AUTHOR INFORMATION

### Corresponding Authors

**Xuefeng Guo** – Center of Single-Molecule Sciences, Institute of Modern Optics, Frontiers Science Center for New Organic Matter, Tianjin Key Laboratory of Micro-scale Optical Information Science and Technology, College of Electronic Information and Optical Engineering, Nankai University, Tianjin 300350, P. R. China; Beijing National Laboratory for Molecular Sciences, National Biomedical Imaging Center, College of Chemistry and Molecular Engineering, Peking University, Beijing 100871, P. R. China; [orcid.org/0000-0001-5723-8528](https://orcid.org/0000-0001-5723-8528); Email: [guoxf@pku.edu.cn](mailto:guoxf@pku.edu.cn)

**Chuancheng Jia** – Center of Single-Molecule Sciences, Institute of Modern Optics, Frontiers Science Center for New Organic Matter, Tianjin Key Laboratory of Micro-scale Optical Information Science and Technology, College of Electronic Information and Optical Engineering, Nankai University, Tianjin 300350, P. R. China; Email: [jiacc@nankai.edu.cn](mailto:jiacc@nankai.edu.cn)

**Jinying Wang** – Center of Single-Molecule Sciences, Institute of Modern Optics, Frontiers Science Center for New Organic Matter, Tianjin Key Laboratory of Micro-scale Optical Information Science and Technology, College of Electronic Information and Optical Engineering, Nankai University, Tianjin 300350, P. R. China; Email: [wangjynk@nankai.edu.cn](mailto:wangjynk@nankai.edu.cn)

**Jingtao Lü** – School of Physics, Institute for Quantum Science and Engineering, Wuhan National High Magnetic Field Center, Huazhong University of Science and Technology, Wuhan 430074, P. R. China; [orcid.org/0000-0001-8518-2816](https://orcid.org/0000-0001-8518-2816); Email: [jtl@hust.edu.cn](mailto:jtl@hust.edu.cn)

**Shan Jin** – Key Laboratory of Pesticide and Chemical Biology, Ministry of Education, College of Chemistry, Central China Normal University, Wuhan 430079, P. R. China;

orcid.org/0000-0002-1070-5456; Email: jinshan@mail.ccnu.edu.cn

## Authors

**Haiyang Ren** – Center of Single-Molecule Sciences, Institute of Modern Optics, Frontiers Science Center for New Organic Matter, Tianjin Key Laboratory of Micro-scale Optical Information Science and Technology, College of Electronic Information and Optical Engineering, Nankai University, Tianjin 300350, P. R. China

**Peihui Li** – Center of Single-Molecule Sciences, Institute of Modern Optics, Frontiers Science Center for New Organic Matter, Tianjin Key Laboratory of Micro-scale Optical Information Science and Technology, College of Electronic Information and Optical Engineering, Nankai University, Tianjin 300350, P. R. China

**Jie Hao** – Beijing National Laboratory for Molecular Sciences, National Biomedical Imaging Center, College of Chemistry and Molecular Engineering, Peking University, Beijing 100871, P. R. China

**Wan Xiong** – School of Physics, Institute for Quantum Science and Engineering, Wuhan National High Magnetic Field Center, Huazhong University of Science and Technology, Wuhan 430074, P. R. China

**Linqi Pei** – Key Laboratory of Pesticide and Chemical Biology, Ministry of Education, College of Chemistry, Central China Normal University, Wuhan 430079, P. R. China

**Boyu Wang** – Center of Single-Molecule Sciences, Institute of Modern Optics, Frontiers Science Center for New Organic Matter, Tianjin Key Laboratory of Micro-scale Optical Information Science and Technology, College of Electronic Information and Optical Engineering, Nankai University, Tianjin 300350, P. R. China

**Cong Zhao** – Center of Single-Molecule Sciences, Institute of Modern Optics, Frontiers Science Center for New Organic Matter, Tianjin Key Laboratory of Micro-scale Optical Information Science and Technology, College of Electronic Information and Optical Engineering, Nankai University, Tianjin 300350, P. R. China

**Suhang He** – Center of Single-Molecule Sciences, Institute of Modern Optics, Frontiers Science Center for New Organic Matter, Tianjin Key Laboratory of Micro-scale Optical Information Science and Technology, College of Electronic Information and Optical Engineering, Nankai University, Tianjin 300350, P. R. China

Complete contact information is available at:

<https://pubs.acs.org/10.1021/acsmaterialslett.5c00047>

## Author Contributions

<sup>†</sup>H.R., P.L., J.H., and W.X. contributed equally to this work. Idea conceptualization: X.G., C.J., and J.W. Experiment: H.R. and P.L. Theoretical analysis: J.H., W.X., J.W., and J.L. Molecule provider: B.W., L.P., and S.J. Supervision: X.G., C.J., and J.W. Writing—original draft: H.R., P.L., C.Z., and S.H. Writing—review and editing: All authors. CRediT: **Haiyang Ren** data curation, formal analysis, project administration, writing - original draft, writing - review & editing; **Peihui Li** data curation, project administration, writing - original draft, writing - review & editing; **Jie Hao** formal analysis, writing - review & editing; **Wan Xiong** formal analysis, writing - review & editing; **Linqi Pei** resources, writing - review & editing; **Boyu Wang** resources, writing - review & editing; **Cong Zhao** writing - original draft, writing - review & editing; **Suhang He**

writing - original draft, writing - review & editing; **Shan Jin** funding acquisition, resources, writing - review & editing; **Jing-Tao Lü** formal analysis, resources, writing - review & editing; **Jinying Wang** supervision, writing - original draft, writing - review & editing; **Chuanheng Jia** conceptualization, data curation, formal analysis, funding acquisition, project administration, resources, supervision, writing - review & editing; **Xuefeng Guo** conceptualization, data curation, formal analysis, funding acquisition, methodology, project administration, resources, supervision, writing - review & editing.

## Notes

The authors declare no competing financial interest.

## ACKNOWLEDGMENTS

We acknowledge primary financial supports from the National Key R&D Program of China (2024YFA1208100, 2021YFA1200102, 2021YFA1200101, 2022YFE0128700 and 2023YFF1205803), the National Natural Science Foundation of China (22173050, 22150013, 21727806, 21933001 and 22072053), Beijing National Laboratory for Molecular Sciences (BNLMS-CXXM-202407) and the Natural Science Foundation of Beijing (2222009).

## REFERENCES

- (1) Mattia, E.; Otto, S. Supramolecular systems chemistry. *Nat. Nanotechnol.* **2015**, *10*, 111–119.
- (2) Neel, A. J.; Hilton, M. J.; Sigman, M. S.; Toste, F. D. Exploiting non-covalent  $\pi$  interactions for catalyst design. *Nature* **2017**, *543*, 637–646.
- (3) Hunter, C. A.; Sanders, J. K. M. The nature of  $\pi$ - $\pi$  interactions. *J. Am. Chem. Soc.* **1990**, *112*, 5525–5534.
- (4) Cockroft, S. L.; Hunter, C. A.; Lawson, K. R.; Perkins, J.; Urch, C. J. Electrostatic control of aromatic stacking interactions. *J. Am. Chem. Soc.* **2005**, *127*, 8594–8595.
- (5) He, S.; Biedermann, F.; Vankova, N.; Zhechkov, L.; Heine, T.; Hoffmann, R. E.; De Simone, A.; Duignan, T. T.; Nau, W. M. Cavitation energies can outperform dispersion interactions. *Nat. Chem.* **2018**, *10*, 1252–1257.
- (6) Liu, Y.; Huang, Y.; Duan, X. Van der Waals integration before and beyond two-dimensional materials. *Nature* **2019**, *567*, 323–333.
- (7) Nerngchamnong, N.; Yuan, L.; Qi, D. C.; Li, J.; Thompson, D.; Nijhuis, C. A. The role of van der Waals forces in the performance of molecular diodes. *Nat. Nanotechnol.* **2013**, *8*, 113–118.
- (8) Aradhya, S. V.; Frei, M.; Hybertsen, M. S.; Venkataraman, L. Van der Waals interactions at metal/organic interfaces at the single-molecule level. *Nat. Mater.* **2012**, *11*, 872–876.
- (9) Zhang, C.; Cheng, J.; Wu, Q.; Hou, S.; Feng, S.; Jiang, B.; Lambert, C. J.; Gao, X.; Li, Y.; Li, J. Enhanced  $\pi$ - $\pi$  stacking between dipole-bearing single molecules revealed by conductance measurement. *J. Am. Chem. Soc.* **2023**, *145*, 1617–1630.
- (10) Tang, Y.; Zhou, Y.; Zhou, D.; Chen, Y.; Xiao, Z.; Shi, J.; Liu, J.; Hong, W. Electric field-induced assembly in single-stacking terphenyl junctions. *J. Am. Chem. Soc.* **2020**, *142*, 19101–19109.
- (11) Li, P.; Hou, S.; Alharbi, B.; Wu, Q.; Chen, Y.; Zhou, L.; Gao, T.; Li, R.; Yang, L.; Chang, X.; Dong, G.; Liu, X.; Decurtins, S.; Liu, S. X.; Hong, W.; Lambert, C. J.; Jia, C.; Guo, X. Quantum interference-controlled conductance enhancement in stacked graphene-like dimers. *J. Am. Chem. Soc.* **2022**, *144*, 15689–15697.
- (12) Wei, Y.; Li, L.; Greenwald, J. E.; Venkataraman, L. Voltage-modulated van der Waals interaction in single-molecule junctions. *Nano Lett.* **2023**, *23*, 567–572.
- (13) Zhou, P.; Fu, Y.; Wang, M.; Qiu, R.; Wang, Y.; Stoddart, J. F.; Wang, Y.; Chen, H. Robust single-supermolecule switches operating in response to two different noncovalent interactions. *J. Am. Chem. Soc.* **2023**, *145*, 18800–18811.

- (14) Wang, Y.; Liu, R.; Zhang, Z.; Wei, J.; Yang, Z. Large optical asymmetry in silver nanoparticle assemblies enabled by CH- $\pi$  interaction-mediated chirality transfer. *J. Am. Chem. Soc.* **2023**, *145*, 4035–4044.
- (15) Song, S.; Wang, L.; Su, J.; Xu, Z.; Hsu, C. H.; Hua, C.; Lyu, P.; Li, J.; Peng, X.; Kojima, T.; Nobusue, S.; Telychko, M.; Zheng, Y.; Chuang, F. C.; Sakaguchi, H.; Wong, M. W.; Lu, J. Manifold dynamic non-covalent interactions for steering molecular assembly and cyclization. *Chem. Sci.* **2021**, *12*, 11659–11667.
- (16) Phipps, R. Cluster preface: non-covalent interactions in asymmetric catalysis. *Synlett* **2016**, *27*, 1024–1026.
- (17) Onneken, C.; Morack, T.; Soika, J.; Sokolova, O.; Niemeyer, N.; Mück-Lichtenfeld, C.; Daniliuc, C. G.; Neugebauer, J.; Gilmour, R. Light-enabled deracemization of cyclopropanes by Al-salen photocatalysis. *Nature* **2023**, *621*, 753–759.
- (18) Sherrill, C. D. Energy component analysis of  $\pi$  interactions. *Acc. Chem. Res.* **2013**, *46*, 1020–1028.
- (19) Hobza, P.; Selzle, H. L.; Schlag, E. W. Potential energy surface of the benzene dimer: ab initio theoretical study. *J. Am. Chem. Soc.* **1994**, *116*, 3500–3506.
- (20) Cubberley, M. S.; Iverson, B. L. <sup>1</sup>H NMR investigation of solvent effects in aromatic stacking interactions. *J. Am. Chem. Soc.* **2001**, *123*, 7560–7563.
- (21) Ehrlich, S.; Moellmann, J.; Grimme, S. Dispersion-corrected density functional theory for aromatic interactions in complex systems. *Acc. Chem. Res.* **2013**, *46*, 916–926.
- (22) Fatima, M.; Steber, A. L.; Poblitzki, A.; Pérez, C.; Zinn, S.; Schnell, M. Rotational signatures of dispersive stacking in the formation of aromatic dimers. *Angew. Chem., Int. Ed.* **2019**, *58*, 3108–3113.
- (23) Li, P.; Zhou, L.; Zhao, C.; Ju, H.; Gao, Q.; Si, W.; Cheng, L.; Hao, J.; Li, M.; Chen, Y.; Jia, C.; Guo, X. Single-molecule nano-optoelectronics: insights from physics. *Rep. Prog. Phys.* **2022**, *85*, 086401.
- (24) Wu, S.; Gonzalez, M. T.; Huber, R.; Grunder, S.; Mayor, M.; Schonenberger, C.; Calame, M. Molecular junctions based on aromatic coupling. *Nat. Nanotechnol.* **2008**, *3*, 569–574.
- (25) Feng, A.; Zhou, Y.; Al-Shebami, M. A. Y.; Chen, L.; Pan, Z.; Xu, W.; Zhao, S.; Zeng, B.; Xiao, Z.; Yang, Y.; Hong, W.  $\sigma$ - $\sigma$  stacked supramolecular junctions. *Nat. Chem.* **2022**, *14*, 1158–1164.
- (26) Zhou, C.; Li, X.; Gong, Z.; Jia, C.; Lin, Y.; Gu, C.; He, G.; Zhong, Y.; Yang, J.; Guo, X. Direct observation of single-molecule hydrogen-bond dynamics with single-bond resolution. *Nat. Commun.* **2018**, *9*, 807.
- (27) Wheeler, S. E. Understanding substituent effects in noncovalent interactions involving aromatic rings. *Acc. Chem. Res.* **2013**, *46*, 1029–1038.
- (28) Jeziorski, B.; Moszynski, R.; Szalewicz, K. Perturbation theory approach to intermolecular potential energy surfaces of van der Waals complexes. *Chem. Rev.* **1994**, *94*, 1887–1930.
- (29) Carter-Fenk, K.; Herbert, J. M. Electrostatics does not dictate the slip-stacked arrangement of aromatic  $\pi$ - $\pi$  interactions. *Chem. Sci.* **2020**, *11*, 6758–6765.
- (30) Horn, P. R.; Mao, Y.; Head-Gordon, M. Defining the contributions of permanent electrostatics, Pauli repulsion, and dispersion in density functional theory calculations of intermolecular interaction energies. *J. Chem. Phys.* **2016**, *144*, 114107.
- (31) Lu, T.; Chen, F. Revealing the nature of intermolecular interaction and configurational preference of the nonpolar molecular dimers (H<sub>2</sub>)<sub>2</sub>, (N<sub>2</sub>)<sub>2</sub>, and (H<sub>2</sub>)(N<sub>2</sub>). *J. Mol. Model.* **2013**, *19*, 5387–5395.
- (32) Fu, T.; Smith, S.; Camarasa-Gómez, M.; Yu, X.; Xue, J.; Nuckolls, C.; Evers, F.; Venkataraman, L.; Wei, S. Enhanced coupling through  $\pi$ -stacking in imidazole-based molecular junctions. *Chem. Sci.* **2019**, *10*, 9998–10002.